

The design and performance of the ATLAS Inner Detector trigger in high pileup collisions at 13 TeV at the Large Hadron Collider

Julie Kirk^{1,*}, on behalf of the ATLAS Collaboration

¹Rutherford Appleton Laboratory, Science and Technology Facilities Council, Harwell Campus, Didcot, OX11 0QX

Abstract. The design and performance of the ATLAS Inner Detector (ID) trigger algorithms running online on the High Level Trigger (HLT) processor farm for 13 TeV LHC collision data with high pileup are discussed. The HLT ID tracking is a vital component in all physics signatures in the ATLAS trigger for the precise selection of the rare or interesting events necessary for physics analysis without overwhelming the offline data storage in terms of both size and rate. To cope with the high interaction rates expected in the 13 TeV LHC collisions, the ID trigger was redesigned during the 2013-15 long shutdown. The performance of the ID trigger in Run 2 data from 13 TeV LHC collisions has been excellent and exceeded expectations, even at the very high interaction multiplicities observed at the end of data-taking in 2017. The detailed efficiencies and resolutions of the ID trigger in a wide range of physics signatures are presented for the Run 2 data. The superb performance of the ID trigger algorithms in these extreme pileup conditions demonstrates how the ID tracking continues to lie at the heart of the trigger performance to enable the ATLAS physics program, and will continue to do so in the future.

1 Introduction

The ATLAS experiment [1] at the LHC [2] is a general purpose detector designed to study a wide range of high- p_T physics. The trigger system [3] is responsible for selecting, in real-time, the events to be recorded and kept for further analysis. For Run 2, starting in 2015, the ATLAS trigger system was upgraded to cope with the higher event rates and larger number of simultaneous proton-proton collisions (pile-up) delivered by the LHC. The Inner Detector (ID) tracking trigger is an essential part of the trigger system and is used to identify many different physics signatures while maintaining manageable recording rates. The improvements made to the ID trigger for Run 2 are described here and performance results from the 2017 and 2018 data-taking are presented.

*e-mail: Julie.Kirk@stfc.ac.uk

From ATL-DAQ-PROC-2018-034. Published with permission by CERN.

2 ATLAS detector and Trigger

ATLAS is a cylindrical detector with an almost complete solid angle coverage around the beam interaction point. The main sub-systems of the detector are the ID, calorimeter and muon systems. The layout of the Inner Detector is shown in Figure 1, illustrating the layers of silicon pixel, strip detectors and straw-tube TRT detectors. The detector covers the azimuthal range $|\eta| < 2.5$. The innermost pixel layer was added for Run 2 to provide more robust track finding and better impact parameter resolution.

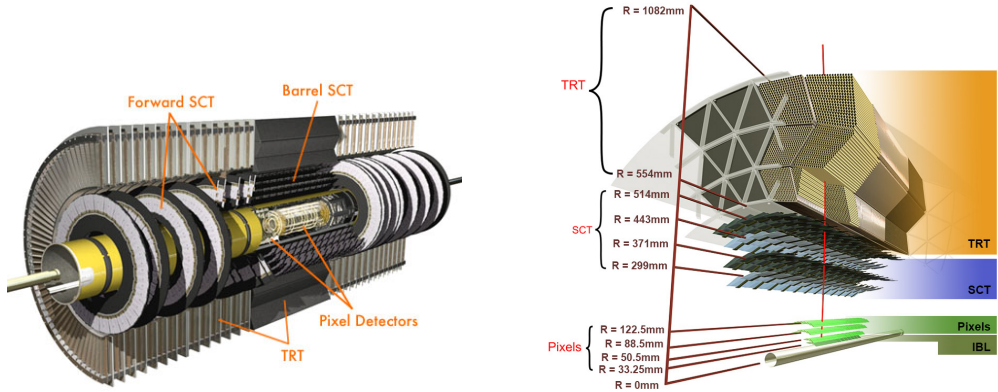


Figure 1. Left: Schematic of the Inner Detector. Right: A segment of the ATLAS ID barrel showing the radial layout of the detector sub-systems.

The ATLAS trigger consists of two levels: the Level-1 hardware trigger and a software-based High Level Trigger (HLT). The Level-1 trigger uses a subset of information from the calorimeter and muon detectors to reduce the event rate from the 40 MHz beam-crossing rate down to about 100 kHz. It identifies Regions-of-Interest (RoIs) in the event and has a latency of $2.5 \mu\text{s}$, after which time events are either rejected or passed on to the HLT. The HLT consists of software algorithms running on a farm of about 40-50 thousand processing slots and selects events at an average rate of 1 kHz. It uses full-granularity detector information to reconstruct features of the event using algorithms close to those used for offline analysis. The HLT can process either the full event or regions of the event defined by the Level-1 RoIs. An important part of the HLT system is the ID tracking trigger which provides track and vertex information to help decide whether or not an event should be accepted.

3 ID Trigger improvements

In Run 1, the HLT software and hardware was divided into two steps, hence there were also two steps of trigger tracking. An initial step used fast software algorithms to provide tracks which could be used to refine the L1 decision. This was followed by a second, precision, step using more offline-like algorithms to further improve object parameters and make a final decision. The ID tracking ran in reduced volume RoI where the spatial size of the region was determined by the physics signature. In order to reconstruct all tracks from some signatures, e.g. taus and b -jets, large RoIs were required leading to high processing times for the trigger tracking in these cases. In Run 2, the two software HLT levels were combined allowing greater flexibility in the design of triggers. For the ID trigger this provided the opportunity to optimise the RoI geometry and employ a multiple stage approach for tau and b -jet triggers.

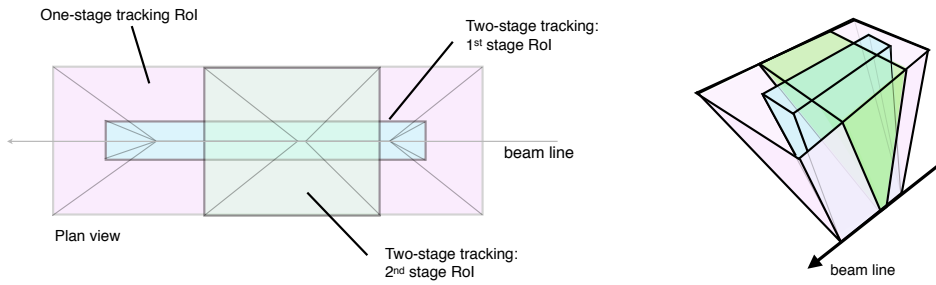


Figure 2. Schematic of the Regions of Interest (RoIs) used for tracking in tau chains in Run 1 (pink) and Run 2 (blue and green). Left: plan view, Right: 3-d view

Figure 2 compares the RoIs used for tau chains in Run 1 and Run 2. In Run 1, a fast track algorithm followed by precision tracking was performed in a single RoI which was long in z , along the beam line, ($\Delta z = 225$ mm) and wide in both η and ϕ ($\Delta\eta \times \Delta\phi = 0.4 \times 0.4$). In Run 2, an initial first stage RoI is defined which is long in z ($\Delta z = 225$ mm) but narrow in η and ϕ ($\Delta\eta \times \Delta\phi = 0.1 \times 0.1$). The fast tracking is performed in this RoI to identify the primary vertex and the track of interest. These are then used to define a second RoI which is short in z ($\Delta z = 10$ mm) but wide in η and ϕ ($\Delta\eta \times \Delta\phi = 0.4 \times 0.4$). Both the fast and precision tracking algorithms are then run in this second RoI. In this way, the tracking algorithms are run in a significantly reduced detector volume compared to Run 1 and this results in a reduction in execution time.

For the jet and b -jet triggers, the reconstruction in the ID trigger runs in three stages - the first stage runs the fast tracking algorithm in very narrow regions about the directions of any jet above 30 GeV, where the regions are fully extended along the beam line (z), to identify tracks above 5 GeV that are then used to identify the primary vertex. The z -position of the vertex is then used to restrict the reconstruction of tracks in each jet to a narrow region in z about the primary vertex, but wider (± 0.4) in both η and ϕ for the second (fast) and third (precision) tracking stages.

Figure 3 shows the processing times of the tracking trigger algorithms for tau chains in the Run 1 and Run 2 different configurations described above. The total mean time for the fast tracking in the two-stage approach used in Run 2 is 44.5 ms corresponding to a fractional saving in processing time with respect to the single-stage tracking of greater than 30%.

4 ID Trigger performance

In this section, the performance for the ID trigger track reconstruction [4] using $\sqrt{s} = 13$ TeV data recorded during 2017 and 2018 is presented. Figure 4 (left) shows the efficiency of track finding as a function of transverse momentum, p_T , for offline medium quality muon candidates. The efficiency is determined using a 24 GeV muon trigger configured to select events using tracks in the muon spectrometer only. Offline muon candidates are required to have at least one pixel hit, at least 4 SCT clusters and no more than two missing hits from the silicon detectors where such hits would be expected. If expected, there should be at least one hit in the innermost pixel layer. For the muon trigger, the ID reconstruction is performed in a single RoI and runs first the fast tracking followed by precision tracking algorithms. The efficiency is close to 100% for all p_T .

Figure 4 (right) shows the track finding efficiency of the ID trigger for tracks from offline medium quality 1-prong tau candidates with offline p_T greater than 20 GeV as a function of

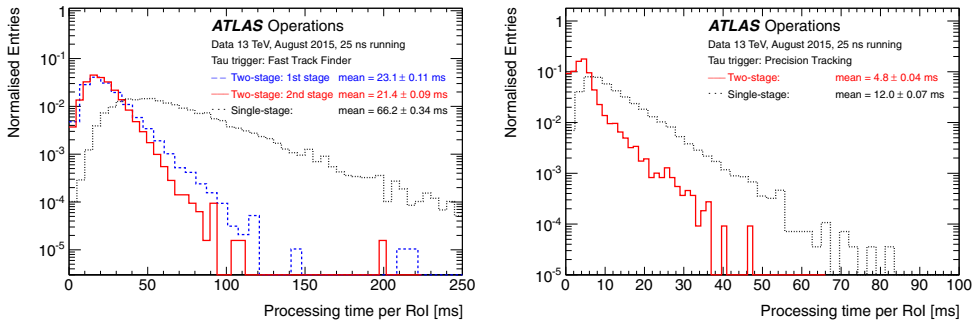


Figure 3. Processing times for the fast tracking (left) and precision tracking (right) algorithms for the tau signature [4]. The single stage approach as used in Run 1 is shown by the black dotted line. The two-stage tracking used in Run 2 is shown by the solid red and dashed blue lines. The data were taken during collisions in August 2015 with the LHC colliding with a 25 ns bunch spacing. The mean number of interactions per bunch crossing was $\langle \mu \rangle \sim 14$.

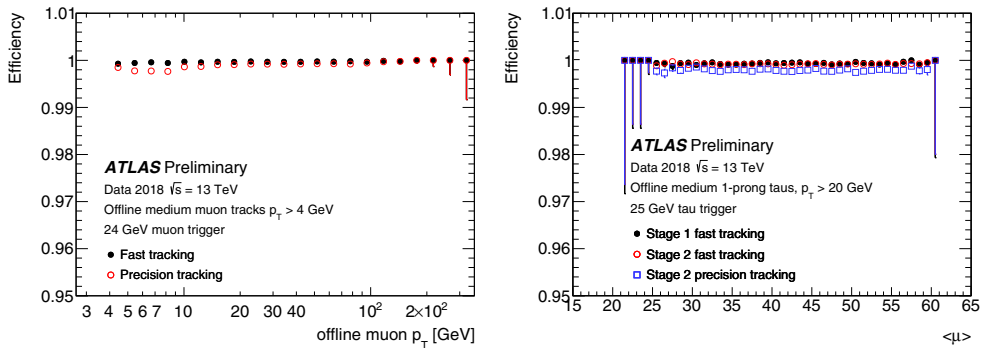


Figure 4. Efficiency of ID trigger track reconstruction for offline medium quality muons as a function of transverse momentum, p_T (left) and offline medium quality 1-prong tau candidates as a function of the mean interaction multiplicity per bunch-crossing (pile-up), $\langle \mu \rangle$ [4]. Statistical, Bayesian uncertainties are shown.

the mean interaction multiplicity per bunch-crossing (pile-up). The efficiency is evaluated with a 25 GeV tau trigger configured to select only on the calorimeter cluster. Offline tracks are required to have no missing hits from those expected in the pixel detector, and a tight overall selection on the total number of silicon hits. The efficiency is close to 100% for all p_T and is flat with increasing pile-up.

Figure 5 shows the track finding efficiency of the ID trigger for tracks with $p_T > 1$ GeV within jets as a function of the offline track p_T (left) and pseudorapidity, η (right). The efficiency is evaluated for the 55 GeV jet trigger. Offline tracks are required to have the same hit requirements as those described above for the muon tracks. The efficiency is once again very high and independent of the level of pile-up.

The track transverse (left) and longitudinal (right) impact parameter resolutions are shown in Figure 6 for tracks with $p_T > 1$ GeV within jets as a function of the offline track pseudorapidity. The impact parameter is defined as the perpendicular distance of closest approach of the track to the primary vertex. The resolution is the difference between the value of the

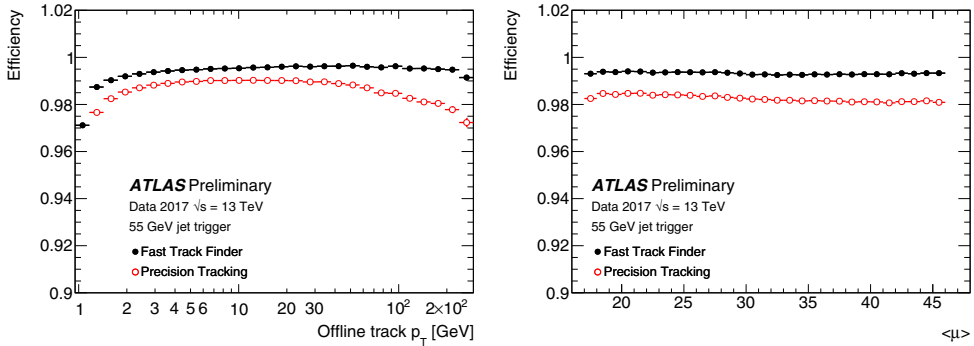


Figure 5. Left: Efficiency for the ID tracking trigger for tracks within jets with $p_T > 1$ GeV as a function of p_T (left) and η (right) [4]. Statistical, Bayesian uncertainties are shown.

impact parameter for online (trigger) and offline tracks. The track selection is the same as for the efficiency plots shown above. The transverse impact parameter resolution is less than $20 \mu\text{m}$ for the precision tracking and less than $25 \mu\text{m}$ for the fast tracking algorithm at central rapidity. For the longitudinal impact parameter, the resolution is approximately $50 \mu\text{m}$ for both algorithms at central pseudorapidity.

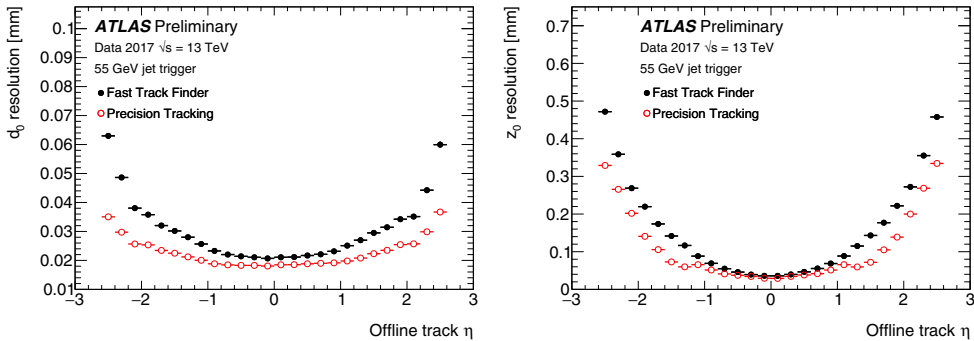


Figure 6. The transverse, d_0 , (left) and longitudinal, z_0 , (right) impact parameter resolutions as a function of offline track pseudorapidity (η) for trigger tracks with $p_T > 1$ GeV within jets [4]. The resolution is evaluated for the 55 GeV jet trigger. Statistical uncertainties are shown.

5 Conclusions

During 2017 and 2018, the LHC delivered record high instantaneous luminosity and pile-up levels. The ATLAS Inner Detector tracking trigger has performed well under these challenging conditions due to improvements made during the preceding Long Shutdown. The performance of the tracking for muons, taus and jets has been shown to be excellent with efficiencies close to 100% and flat with pile-up.

References

- [1] ATLAS Collaboration, JINST 3 **The ATLAS Experiment at the CERN Large Hadron Collider**, S08003 (2008)
- [2] L. Evans and P. Bryant, JINST 3 **LHC Machine**, S08001 (2008)
- [3] ATLAS Collaboration, Eur. Phys. J C 77 **Performance of the ATLAS Trigger system in 2015**, 317 (2017)
- [4] ATLAS Collaboration, **HLT Tracking Public results**
<https://twiki.cern.ch/twiki/bin/view/AtlasPublic/HLTTrackingPublicResults>